CMLS, Cell. Mol. Life Sci. 61 (2004) 2998–3007
1420-682X/04/232998-10
DOI 10.1007/s00018-004-4318-2

CMLS Cellular and Molecular Life Sciences

Research Article

Modulation of signal transduction through the cellular prion protein is linked to its incorporation in lipid rafts

B. Hugel[a, b, *], M. C. Martínez[a, b], C. Kunzelmann[a, b], T. Blättler[c], A. Aguzzi[c] and J.-M. Freyssinet[a, b]

[a] Institut d'Hématologie et d'Immunologie, Université Louis Pasteur, Faculté de Médecine, 4 rue Kirschleger, 67085 Strasbourg (France), Fax: +33 (0)3 90 24 40 16, e-mail: Benedicte.Hugel@hemato-ulp.u-strasbg.fr
[b] Unité 143 INSERM, Bâtiment Gregory Pincus, 80 rue du Général Leclerc, 94276 Le Kremlin-Bicêtre Cedex (France)
[c] Institut für Neuropathologie, Universitätsspital Zürich, Schmelzbergstrasse 12, 8091 Zurich (Switzerland)

Received 22 July 2004; received after revision 10 September 2004; accepted 7 October 2004

Abstract. Because expressed at a significant level at the membrane of human T cells, we made the hypothesis that the cellular prion protein (PrP^c) could behave as a receptor, and be responsible for signal transduction. PrP^c engagement by specific antibodies was observed to induce an increase in cytosolic calcium concentration and led to enhanced activity of Src protein tyrosine kinases. Antibodies to CD4 and CD59 did not influence calcium fluxes or signaling. The effect was maximal after the formation of a network involving avidin and biotinylated antibody to PrP^c and was inhibited after raft disruption. PrP^c localization was not restricted to rafts in resting cells but engagement was a prerequisite for signaling induction, with concomitant PrP^c recruitment into rafts. These results suggest a role for PrP^c in signaling pathways, and show that lateral redistribution of the protein into rafts is important for subsequent signal transduction.

Key words. Cross-linking; rafts; Src protein tyrosine kinases; signal transduction.

The cellular prion protein (PrP^c) is a glycosyl-phosphatidylinositol (GPI)-anchored cell surface protein [1, 2] expressed by neural cells and a wide range of other tissues including vascular and circulating blood cells [3], hematopoietic cells [4], and the lymphoreticular system [5]. Whereas its implication in transmissible spongiform encephalopathies is generally accepted, its physiological role remains unknown, and gene knockout experiments have not produced a clear phenotype [6–8]. The pathology is attributed to accumulation of an abnormally folded form of the protein in the central nervous system, with probable participation of the lymphoreticular system in the early stages of neuroinvasion [9]. PrP^c-null mice do not show immune deficiency, and do not develop prion disease [2, 10], but this does not rule out the participation of the lymphoid system in the transmission of the disease. PrP^c may participate in lymphocyte activation [11], and its level of expression at the T cell surface is up-regulated as a consequence of cellular activation [12].

GPI-linked proteins are known to be preferentially localized in membrane structures that are detergent resistant under particular conditions and rich in sphingolipids and cholesterol [13]. Such domains, termed rafts, are supposed to be instrumental in the recruitment of specialized proteins for intracellular signal transduction because of the presence of signaling molecules such as heterotrimeric G proteins and Src family tyrosine kinases at their extension in the cytoplasmic leaflet of the membrane [14]. In T lymphocytes, T cell receptor (TCR)-mediated Ca^{2+} influx is inhibited after raft disruption showing the requirement for raft integrity for efficient T cell activation [15]. Among the various Ca^{2+} sources, Ca^{2+} influx through

* Corresponding author.

store-operated Ca^{2+} channels is normally sustained during T lymphocyte activation [16]. Store-operated Ca^{2+} entry (SOCE) is triggered by the depletion of endoplasmic reticulum Ca^{2+} stores, which evokes the secondary opening of plasma membrane Ca^{2+} channels, allowing subsequent Ca^{2+} influx [17]. Although the intracellular mechanisms responsible for SOCE activation are mostly unknown, SOCE seems to be involved in phosphorylation cascades and coupling between the endoplasmic reticulum and the plasma membrane [18–20]. Modulation of Ca^{2+} fluxes following PrP^c engagement would therefore be indicative of an involvement in signal transduction.

PrP^c expression levels by human T lymphocytes are high, comparable to those of CD3 or CD4, and dependent on the cell activation state [11, 12]. PrP^c is known to be concentrated in raft domains in several cell types, including murine neurons and ScN2a cells [21–23]. Most studies on the PrP^c protein have been carried out on brain tissues or neuronal cell lines, but little is known about its distribution at the cell surface in cells of non-neuronal origin.

The aim of the present study was to assess the effects of PrP^c engagement and recruitment into rafts and their implication in signal transduction in CEM-T cells. For this, we examined Ca^{2+} flux modulations following engagement using anti-PrP^c antibodies (Abs). As illustrated by studies of the TCR-mediated signaling [24–26], antigen cross-linking by corresponding Abs has proved efficient to elicit a cellular response, especially in the absence of known ligand. Immunological labeling and Western blot analysis of sucrose density gradient fractions were performed to assess PrP^c localization with respect to rafts at the surface of human lymphoid CEM-T cells.

Materials and Methods

The polyclonal goat anti-human PrP (GaHPrP) Ab was from Chemicon (Temecula, Calif.). The monoclonal anti-human PrP (3F4) was prepared according to Kascsak et al. [27]. The 6H4 anti-PrP Ab was from Prionics (Schlieren, Switzerland), the activation-specific Ab directed to the phosphorylated site P418 of Src family protein tyrosine kinases was from BioSource International (Camarillo, Calif.), horseradish peroxidase (HRP)-conjugated anti-rabbit Ab was from Jackson ImmunoResearch (West Grove, Pa.), and HRP-conjugated anti-goat Ab was from Tebu-bio (Le Perray en Yvelines, France). The biotinylated anti-CD4 and biotinylated control Abs were from Leinco Technologies (Ballwin, Mo.). The anti-CD59 Ab and rabbit anti-Fyn Ab were from Santa Cruz Biotechnology (Santa Cruz, Calif.). Protein A Sepharose was purchased from Pharmacia Biotech (Uppsala, Sweden). The 3F4 and anti-CD59 Abs were biotinylated following the procedure described by Aupeix et al. [28]. Phosphatidylinositol-specific phospholipase C (PIPLC), methyl-β-cyclodextrin (MβCD), and avidin were from Sigma (St. Louis, Mo.).

Cell culture

Human lymphoid CEM-T cells were cultured in X-VIVO 15 serum-free medium at 37 °C in a humidified 5% CO_2 atmosphere at a density of 5×10^5 cells/ml. Absence of mycoplasma contamination was controlled.

Cell treatment with anti-PrP Ab and cross-linking

The polyclonal GaHPrP Ab was dialyzed before use against Tris buffer to remove thimerosal preservative. As a control, we used dialyzed goat serum. Fifteen microliters was added to 10^6 cells.

For treatments using monoclonal Abs, 10 µg was added to 10^6 cells (20 µg/ml final concentration). Biotinylated IgG2a isotype was the negative control for biotinylated 3F4 and anti-CD4-biotin. Biotinylated IgG1 isotype was the negative control for biotinylated anti-CD59.

Abs were incubated for 45 min at 37 °C with the cells. For calcium measurements, Fluo-3/acetoxymethyl ester (Fluo-3; 3 µM) was added during the last 30 min, at room temperature, in the dark. Values reported in the Results section are differences observed with PrP^c-specific versus control Abs. Results obtained in the presence of control Abs were not significantly different from values corresponding to non-treated cells (data not shown).

Cross-linking of biotinylated Abs was achieved after the 45-min preincubation at 37 °C with the Ab of interest (10 µg for 10^6 cells, 20 µg/ml final concentration). Cells were then centrifuged for 3 min at 12,000 g and resuspended in X-VIVO 15 at 10^6 cells/ml. Avidin (100 µg for 10^6 cells, 100 µg/ml final concentration) and Fluo-3 were then added and left in contact with the cells for 30 min, at room temperature, in the dark. As a negative control, avidin alone was used, and values obtained under these conditions were not significantly different from values corresponding to non-treated cells. Cells were centrifuged again and resuspended in X-VIVO 15 medium (1.8 mM Ca^{2+}) just before induction of Ca^{2+} responses by A23187 Ca^{2+} ionophore (2 µM) or thapsigargin (TG; 1 µM) treatments (see below).

Measurements of $[Ca^{2+}]_i$ by flow cytometry

To study Ca^{2+} release and Ca^{2+} entry separately, 2 mM EGTA was added to chelate Ca^{2+} present in X-VIVO 15 medium 5 min before TG treatment (1 µM) and a 2 mM Ca^{2+} concentration was then restored to allow SOCE. Fluo-3 fluorescence was monitored using a FACScan flow cytometer and the CELLQuest software (Becton-Dickinson, Palo Alto, Calif.). A baseline value was obtained for each sample by fluorescence measurement for 30 s before addition of pharmacological agents. Collection was immediately resumed, then terminated after an

additional 5–10 min (~50,000 events). Fluo-3 fluorescence was expressed in arbitrary fluorescence units and plotted as FL-1 versus time. Fluorescence intensities were expressed as the increase in fluorescence with respect to baseline fluorescence intensity before stimulation.

Western blotting of Src tyrosine kinases

Western blotting was performed to investigate the activation of Src family protein tyrosine kinases following PrP^c engagement. A23187 or TG were not added in immunoblotting experiments. For control purposes, PIPLC or MβCD treatments (30 min at 37 °C or 10 min at 37 °C, respectively) were performed before exposure of the cells to the 3F4-biotin Ab, in order to show the respective dependence of the activation of the Src kinases on the presence of GPI-linked proteins, including PrP^c, and on raft integrity. Cells were pelleted, washed once with Tris buffer and solubilized for 30 min at 4 °C in lysis buffer consisting of 50 mM Tris buffer containing 8 mM $MgCl_2$, 5 mM EGTA, 0.5 mM EDTA, 10 µg/ml of leupeptin, pepstatin and aprotinin, 1 mM PMSF, 250 mM NaCl, 1% (v/v) Triton X-100, and the phosphatase inhibitor Na_3VO_4 (1 mM) adjusted to pH 7.2. After 3 min centrifugation at 12,000 g, the supernatant was frozen and protein determination was made using the Bradford method. Samples containing 60 µg protein were separated on 7.5% SDS-PAGE. Separated proteins were then blotted onto Protran nitrocellulose membrane and blots were probed with the activation-specific Ab directed to the phosphorylated site P418 of Src tyrosine kinases. Development was achieved with the appropriate HRP-conjugated secondary Ab and bound Abs were detected by chemiluminescence. Reprobing of blots with an anti-β-actin Ab was performed in all experiments to make sure that differences observed were not due to differences in the quantity of loaded protein.

In another set of experiments, Western blots were performed with samples obtained after immmunoprecipitation using the anti-Fyn polyclonal Ab. Briefly, after a 'preclear' step using 0.25 µg rabbit control IgG and 20 µl protein A Sepharose, 400 µg protein was immunoprecipitated with 5 µg anti-Fyn Ab and captured using 50 µl protein A Sepharose. After three washing steps, the pellet was resuspended in 60 µl electrophoresis sample buffer and boiled for 5 min. The supernatant was then subjected to SDS-PAGE and transferred for blotting. Immunoblotting using the SrC P418$^+$ Ab was then carried out to specifically reveal activated Fyn. Reprobing of the blot was performed with the anti-Fyn Ab to control for the quantity of loaded protein.

Sucrose density gradients and Western blotting of PrP^c

After preincubation of cells (20×10^6) in the presence of 3F4-biotin Ab + avidin, they were washed once with HBSS and pelleted. The pellets were resuspended in 0.3 ml ice-cold TNE buffer (Tris/HCl buffer, pH 7.2, 158 mM NaCl, 1 mM EGTA), containing protease and phosphatase inhibitors (5 µg/ml leupeptin, 5 mM benzamidine, 1 mM phenylmethylsulfonyl fluoride, 1 mM Na_3VO_4) and 1% Triton X-100. Cells were lysed by three freezing-thawing steps, and intact cells were removed by centrifugation at 12,000 g for 5 min. The cell lysates (0.3 ml) were transferred to the bottom of centrifuge tubes and 0.3 ml of an 80% (w/v) sucrose solution was then added giving a 0.6-ml solution with 40% (w/v) sucrose content. Next, 1.8 ml of 30% sucrose and 1.2 ml of 5% sucrose were successively layered on top of the 40% sucrose solution. The tubes were centrifuged at 200,000 g for 20 h at 4 °C in a Beckman SW41 rotor. Twelve fractions (0.3 ml each) were collected from the top, and the proteins were stored at –20 °C before analysis by Western blotting. Forty microliters of each of the fractions was used for 12% SDS-PAGE. Separated proteins were then blotted onto Protran nitrocellulose membrane and blots were probed with the polyclonal GaHPrP Ab (1:5000). Development was achieved with the HRP-conjugated anti-goat Ab (1:10,000) and bound Abs were detected by chemiluminescence.

Identification of rafts, and PrP^c distribution at the surface of CEM-T cells by fluorescence microscopy

In another set of experiments, rafts and PrP^c distribution were analyzed before or after cross-linking of the PrP^c protein by 3F4-biotin + avidin treatment (in the absence of Fluo-3). Cells were incubated for 45 min at 37 °C with the biotinylated 3F4 Ab (10 µg for 10^6 cells, 20 µg/ml final concentration), centrifuged for 3 min at 12,000 g, and then resuspended in X-VIVO 15 at 10^6 cells/ml. Avidin (100 µg for 10^6 cells, 100 µg/ml final concentration) was then added and incubated for 30 min at room temperature. Cells were centrifuged again and resuspended in X-VIVO 15 medium just before PrP^c labeling using the 6H4 Ab (2 µg for 10^6 cells, 2 µg/ml final concentration). After 90 min at room temperature, cells were centrifuged again, resuspended in HBSS and Fab'_2 goat anti-mouse IgG-phycoerythrin Ab (5 µl for 10^6 cells) was added for 20 min at room temperature. Cholera toxin-FITC (3 µg for 10^6 cells, 3 µg/ml final concentration) was then added for 10 min at room temperature to label GM_1 ganglioside in rafts. Cells were finally washed and resuspended in 10 µl HBSS. PrP^c (red) and rafts (green) were visualized by fluorescence laser scanning microscopy using Spot software from Diagnostic Instruments (Sterling Heights, Mich.).

Statistical analysis

Different antibody treatments were compared using a Mann-Whitney test. Results were considered significant when $p < 0.05$.

Results

The aim of the studies of Ca^{2+} fluxes after anti-PrP treatment of CEM-T cells was to evaluate whether membrane-bound PrP^c could participate in signal transduction. For this, Fluo-3 fluorescence variations were measured by flow cytometry as previously described [29, 30]. The global Ca^{2+} response was evaluated after Ca^{2+} ionophore treatment. To study Ca^{2+} release and Ca^{2+} entry separately, T cells were first exposed to EGTA, and treated with TG which induces Ca^{2+} release from intracellular stores. Ca^{2+} was then reintroduced into the medium to restore the extracellular Ca^{2+} concentration allowing SOCE. As shown in figure 1A (left panel), Ca^{2+} ionophore treatment in the presence of extracellular Ca^{2+} resulted in an increase of $[Ca^{2+}]_i$ within a few seconds. An example for Ca^{2+} release and consecutive SOCE is shown in figure 1B (left panel).

PrP^c engagement modifies A23187 ionophore-induced Ca^{2+} entry

The A23187 ionophore-induced Ca^{2+} response was significantly modified following anti-PrP treatment of CEM-T cells (fig. 2). PrP^c engagement was achieved by treating CEM-T cells with an Ab to this protein. The 3F4 monoclonal Ab and its biotinylated form (3F4-Bi) were responsible for a decrease in Ca^{2+} entry (6 ± 0.9% and 6 ± 0.8%, respectively; n=9) whereas 3F4-Bi + avidin treatment was responsible for a clear augmentation of the flux (12 ± 1.2%, n=9; for an illustration, see also fig. 1A, right panel). Under these conditions, polyclonal GaHPrP^c Ab had no effect on the Ca^{2+} ionophore-induced signal (n=9). The different effects of anti-PrP^c Abs may be related to epitope differences. Anti-CD4-biotin and anti-CD59-biotin treatments did not modify the Ca^{2+} response induced by A23187, even when cross-linking with avidin was performed (n=4; fig. 2).

The Ca^{2+} ionophore A23187 has been shown to induce intracellular Ca^{2+} store depletion and subsequent SOCE [31–33]. In this context, we can reasonably assume that the effects of the different cross-linkings on the A23187-induced Ca^{2+} response are relevant to Ca^{2+} entry mediated by store depletion or to Ca^{2+} release from intracellular stores.

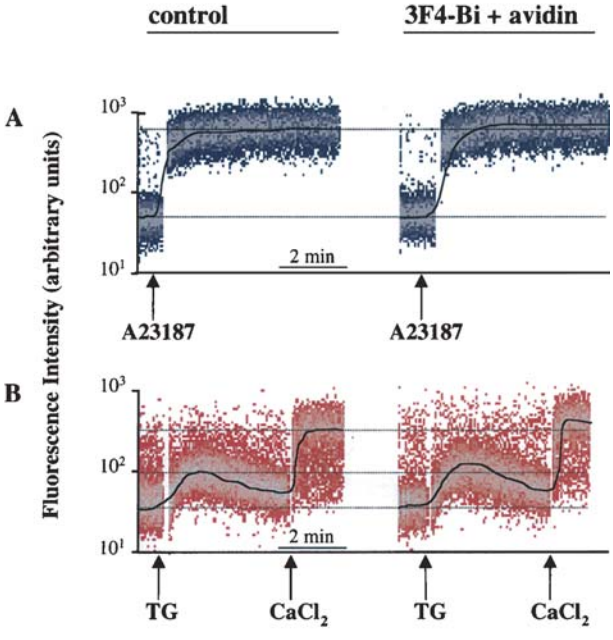

Figure 1. Induction of Ca^{2+} fluxes in CEM-T cells and effect of PrP^c cross-linking. Stimulation of CEM-T cells using ionophore was responsible for an augmentation of the intracellular $[Ca^{2+}]$ which was further enhanced (+11% in this example) by PrP^c cross-linking using a (3F4-Bi + avidin) treatment (*A*). CEM-T cells were also stimulated by TG in the presence of EGTA to induce the release of intracellular Ca^{2+} stores. The reintroduction of Ca^{2+} in the external medium induced SOCE. These two types of Ca^{2+} fluxes were enhanced by (3F4-Bi + avidin) cross-linking treatment (+10% and +31%, respectively, in this example) (*B*). Solid lines represent the averaged and smoothed data as a function of time. Note that scales are logarithmic.

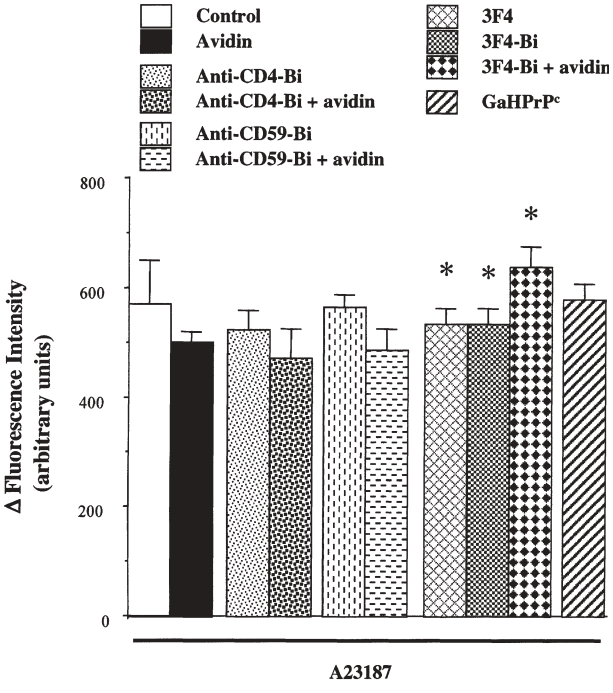

Figure 2. Effect of PrP^c engagement on the Ca^{2+} ionophore-induced Ca^{2+} signal. The Ca^{2+} response was measured after treatment with 2 µM A23187 Ca^{2+} ionophore in the presence of 2 mM Ca^{2+} in the external medium. The 3F4 Ab is a monoclonal Ab, GaHPrP is a polyclonal Ab that may bind different epitopes in the protein and therefore induce a lateral movement of the PrP^c. Treatment combining the biotinylated Ab and avidin is supposed to induce lateral redistribution of PrP^c through cross-linking in an avidin-biotin network. Anti-CD4 and anti-CD59 Abs are both monoclonal. The cross-linking of PrP^c was responsible for an elevation of Ca^{2+} entry, whereas treatments with 3F4 alone led to a decreased response. Neither of the anti-PrP^c polyclonal Abs nor anti-CD4 or anti-CD59 treatments had any effect. Bars are SE. *p* values were determined by the Mann-Whitney test. *$p < 0.05$, n=9 for anti-PrP^c experiments, and n=4 for anti-CD4 and anti-CD59 experiments.

PrP^c engagement enhances Ca^{2+} release from intracellular stores after TG treatment in the presence of EGTA

3F4 and 3F4-Bi were responsible for an augmentation of Ca^{2+} release of 11 ± 5% and 11 ± 1.1%, respectively, after TG treatment in the presence of EGTA (n=12; fig. 3). PrP^c engagement by the polyclonal GaHPrP^c Ab led to a 14 ±1.5% increase in Ca^{2+} release, and 3F4-Bi treatment followed by avidin-induced cross-linking resulted in a more pronounced effect (16 ± 1.1%; n=12; see also fig. 1B, right panel, for an illustration). Avidin alone had no effect on TG-induced Ca^{2+} release from intracellular stores. None of the Ab treatments was capable of triggering Ca^{2+} release by itself (not shown), but Ca^{2+} movements were indeed modulated by all of the anti-PrP^c treatments. Treatments likely to induce network formation (GaHPrP^c and 3F4-Bi + avidin) were responsible for the most pronounced effects, which may be linked to a lateral reorganization of PrP^c molecules at the cell surface. Again, anti-CD4 and anti-CD59 were incapable of inducing any modulation of Ca^{2+} release (n=4).

PrP^c protein engagement augments SOCE

Ca^{2+} restoration after mobilization of intracellular stores using TG in the presence of EGTA leads to Ca^{2+} entry through store-operated Ca^{2+} channels. This mechanism is referred to as SOCE. PrP^c engagement was followed by an augmentation of this particular form of Ca^{2+} entry (fig. 3). The increase was 9 ± 0.8% for 3F4, 9 ± 1.6% for 3F4-Bi, 13 ± 1.5% for GaHPrP^c, and 20 ± 2% for 3F4-Bi + avidin treatment (n=12). Avidin alone, anti-CD4-biotin and anti-CD59-biotin did not significantly modify SOCE (n=4). Again, an augmentation of Ca^{2+} responses was observed after PrP^c engagement, and the effect was more pronounced when treatments induced lateral segregation of the PrP^c protein (for an example, see also fig. 1B, right panel).

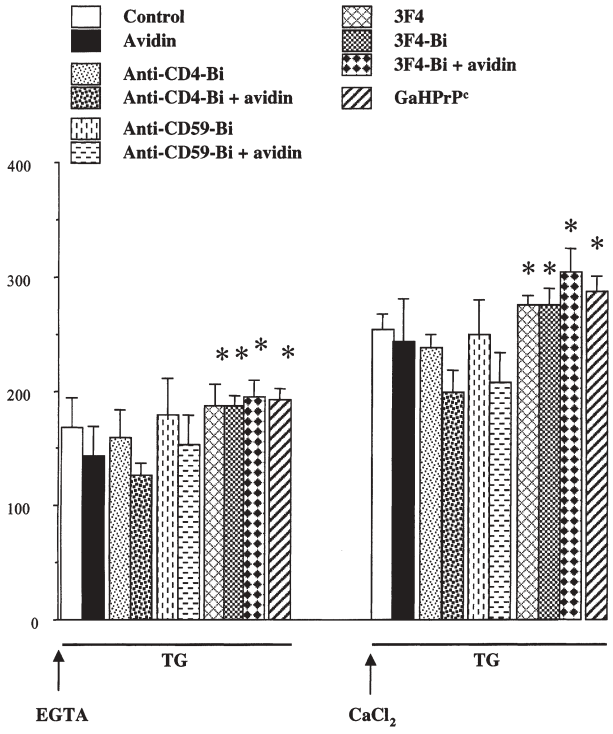

Figure 3. Effect of PrP^c engagement on Ca^{2+} release from intracellular stores and store-operated Ca^{2+} entry. The release of Ca^{2+} from the endoplasmic reticulum stores was induced by TG treatment of the cells 5 min after chelation of extracellular Ca^{2+} by EGTA. SOCE was observed after restoration of a 2 mM Ca^{2+} concentration following TG treatment in the presence of EGTA. Fluo-3 fluorescence was monitored to evaluate variations in the cell responses induced by anti-PrP^c, anti-CD4, and anti-CD59 treatments. Note that all the anti-PrP^c Ab treatments induced an elevation in Ca^{2+} release from intracellular stores, and the effect was more important when the treatment was susceptible to induce lateral protein segregation in the membrane. Anti-CD4 and anti-CD59 Ab treatments had no effect. Bars are SE. *p* values were determined by the Mann-Whitney test. *$p < 0.05$, n=12 for anti-PrP^c experiments, and n=4 for anti-CD4 and anti-CD59 experiments.

PrP^c engagement and activation of Src protein tyrosine kinases

Western blot analysis was performed to investigate the activation of Src tyrosine kinases following 3F4-Bi or 3F4-Bi + avidin treatment of CEM-T cells. An Ab that recognizes the activation-specific phosphorylation site 418 was used. The intensity of the P418$^+$ band of Src family proteins was augmented in CEM-T cells treated with 3F4-Bi compared to non-treated cells (fig. 4B). As previously observed for Ca^{2+} responses, phosphorylation of Src family members was further enhanced when avidin was present (fig. 4B). The molecular weight corresponding to the signal was close to 63 kDa. However, this was not sufficient to clearly indicate the Src family member(s) involved, because Src, Lyn, Fyn, and Lck have molecular weights ranging between 53 and 60 kDa. Because PrP^c was previously shown to be associated with Fyn [34], we tentatively performed a Western blot analysis using the activation-specific Ab after Fyn immunoprecipitation. Fyn was not activated after anti-PrP^c treatment of the cells (fig. 4C). These results show that PrP^c engagement leads to the activation of a member of the family of Src kinases (possibly Lyn, Src, or Lck), which is more pronounced when a lateral movement of PrP^c molecules is induced in an avidin network.

For control purposes, Western blot analysis was also carried out with cells treated with avidin only. No activation of Src kinases could be detected (fig. 4A). Cells were also preincubated with PIPLC before 3F4-Bi + avidin treatment. A clearly diminished PrP^c labeling of CEM-T cells treated with PIPLC was verified by flow cytometry (not shown). Src kinase activation was indeed abolished in a situation where PrP^c protein was removed from the cell surface (fig. 4D). This confirms that the entity responsible for the transfer of biological information is PrP^c itself.

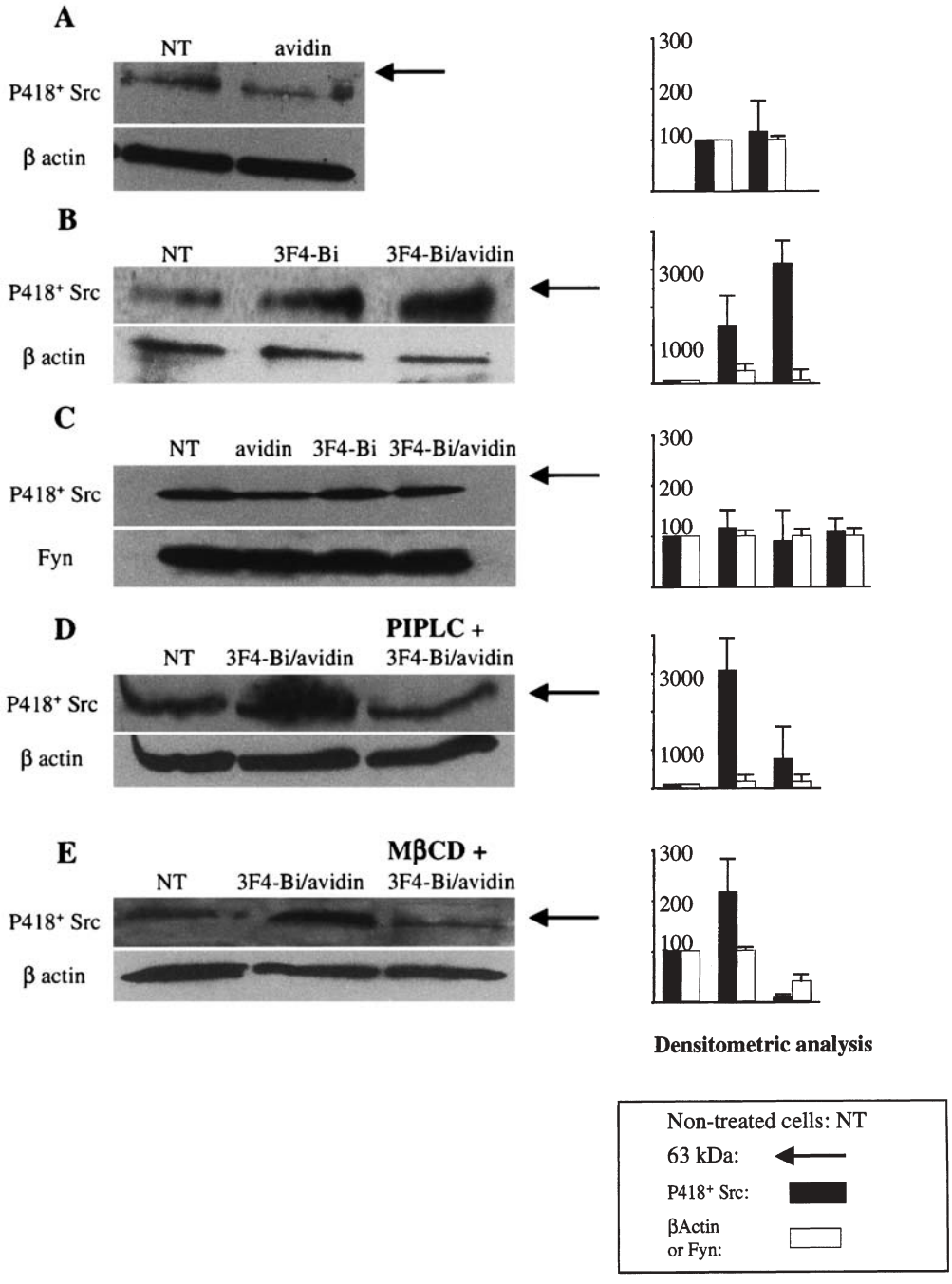

Figure 4. Effect of PrP^c engagement on Src family kinase activity. Western blot analysis was performed using an activation-specific Ab directed to the phosphorylated site P418 of the kinases of the Src family. To study Fyn phosphorylation, an immunoprecipitation step using an anti-Fyn Ab was performed before Western blotting. Sixty micrograms protein (determined using the Bradford method) was loaded in each well. (*A*) Treatment of the cells with avidin alone was not responsible for activation of the Src family kinases. (*B*) Src family kinase activation was detectable after PrP^c engagement (3F4-Bi treatment), and was augmented by an additional cross-linking with avidin. The activation increased when lateral segregation of PrP^c was induced. (*C*) Fyn phosphorylation was not enhanced following PrP^c engagement. (*D*) Activation was abolished when GPI-linked proteins were removed from the cell surface by PIPLC treatment. (*E*) Activation was abolished when raft structures were disrupted after exposure of cells to MβCD, a non-invasive cholesterol acceptor.

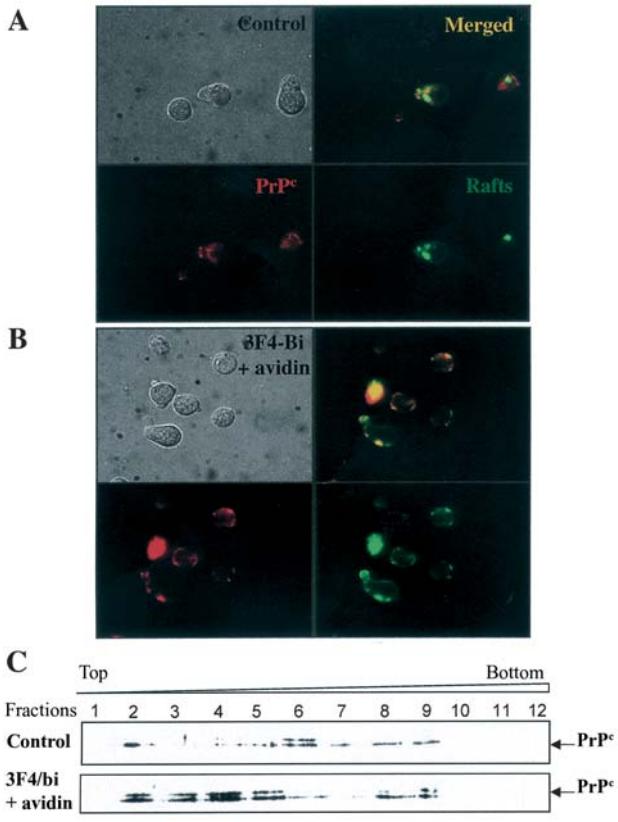

Figure 5. Localization of rafts and PrP^c at the surface of CEM-T cells. Rafts were labeled using cholera toxin-FITC (green) which binds the GM_1 ganglioside. PrP^c was labeled using 6H4 Ab and a secondary Fab'_2 goat anti-mouse IgG-phycoerythrin Ab (red). (*A*) In non-treated CEM-T cells, only 33% (± 0.6%) of resting cells presented a colocalization of PrP^c and GM_1 ganglioside, a raft marker. Note the clear separation between PrP^c and raft labeling in the upper-right quadrant. (*B*) In CEM-T cells treated with 3F4-Bi + avidin, PrP^c and rafts shared the same localization in 65% (± 0.5%) of the cells. In the upper-right picture, the merger of the two colors leads to yellow. (*C*) Western blot analysis of Triton X-100-extracted proteins from CEM-T cells. Cells were incubated in the absence or presence of 3F4-bi Ab + avidin, and subjected to lysis in TNE buffer containing 1% Triton X-100, homogenization, and sucrose density gradient centrifugation. The proteins of each fraction were separated by SDS-PAGE and immunoblotted with the polyclonal GaHPrP Ab. Cross-linking of PrP^c molecules in an avidin network induced the recruitment of PrP^c into rafts.

The raft dependence of the activation of Src tyrosine kinases was assessed by destabilizing such structures before 3F4-Bi + avidin treatment using MβCD, a non-invasive cholesterol acceptor [35]. Src kinase activation was clearly inhibited, emphasizing the requisite for raft integrity in PrP^c-dependent signal transduction (fig. 4E).

PrP^c redistribution from non-raft regions to rafts after 3F4-Bi + avidin treatment

In non-treated CEM-T cells (fig. 5A), only 33% (± 0.6%) of resting cells presented a colocalization of PrP^c and GM_1 ganglioside, a raft marker [36]. In CEM-T cells treated with 3F4-Bi + avidin, the proportion of cells with colocalization was raised ≈ two-fold (65 ± 0.5%, $p < 0.0001$; fig. 5B). Percentages were determined from five different experiments and 50 pictures for each treatment.

To confirm these results, Western blot analysis of fractions obtained by sucrose density gradient centrifugation of non-treated and 3F4-Bi + avidin-treated CEM-T cells was performed. Detergent resistant membrane fragments were found in the 5–30% zone (fractions 3–7). In the presence of 3F4-Bi + avidin (fig. 5C), PrP^c protein was mainly found in fractions 3–5, as indicated by the increase of the PrP^c band in the raft fractions compared to corresponding fractions from non-treated cells. As already reported [11], detection of PrP^c by Western blot reveals several bands with different molecular weight corresponding to different glycosylated forms of the PrP^c protein. The results obtained in the present study suggest that two isoforms of PrP^c are detected in the fractions obtained from CEM-T cells.

Collectively, these observations suggest that the cross-linking of PrP^c, here in an avidin network, leads to the displacement of a significant proportion of PrP^c molecules into raft structures.

Discussion

Several functions, most of them concerning the brain, have already been proposed for PrP^c, including an anti-oxidant potential [37], the control of sleep patterns [38], or involvement in synaptic activity [39]. We propose that the ubiquitous expression of the protein could be indicative of more fundamental roles, relevant to not only the neuronal context. Owing to significant expression levels by lymphocytic cells [12], PrP^c participation in signal transduction was assessed here. The transduction of neuroprotective signals through a cAMP/PKA-dependent pathway has been reported by other investigators [40]. Mouillet-Richard et al. [41] have also observed the modulation of Fyn kinase activity after Ab-mediated cross-linking of the PrP^c in a neuronal differentiation model.

Although PrP^c protein has been shown to be involved in signal transduction in T lymphocytes [11, 42], little is known about its recruitment into rafts and the consequences for T cell activation. Our investigation with CEM-T cells showed that (i) intracellular Ca^{2+} fluxes can be significantly modified upon PrP^c engagement, (ii) activation of Src protein tyrosine kinases can be induced by PrP^c engagement, (iii) raft integrity is essential for subsequent Src tyrosine kinase activation, (iv) in resting CEM-T cells, PrP^c is mainly localized out of the rafts, and (v) effects of PrP^c engagement on signaling pathways are increased when the cells are treated to induce the recruitment of PrP^c molecules into raft structures.

Treatments using anti-PrP^c Abs were chosen in a context where no specific ligand for the PrP^c protein has as yet

been identified. The highest effects were observed after cross-linking with avidin and with polyclonal Abs rather than monoclonal Abs alone suggesting that a relevant physiological ligand would be more efficient if multivalent. Whether the scrapie isoform of the PrP protein could be such a ligand when polymerized in amyloid fibers remains an open question.

Although modulation of Ca^{2+} movements was observed with all of the anti-PrP^c Ab treatments, the corresponding responses were different. While Abs that do not induce formation of a network (3F4 and 3F4-Bi) gave rise to inhibitory effects of the calcium response induced by ionophore, they enhanced the release of Ca^{2+} from internal stores and SOCE after restoration of external Ca^{2+}. Treatments inducing network formation (GaHPrP^c and 3F4-Bi + avidin) were indeed responsible for enhanced effects, linked to a lateral reorganization of PrP^c molecules at the cell surface. These differences were probably due to the existence of several complementary intracellular mechanisms involved in the regulation of calcium movements induced by various agents.

Treatments using Abs to CD4 (transmembrane) and to CD59 (GPI-linked), both reported to be mainly localized in rafts [43], did not induce Ca^{2+} signaling in CEM-T cells even though CD4 was previously shown to be involved in signaling [44] and CD59 to be responsible for cell death induction in Jurkat T cells [45]. These observations demonstrate that neither raft localization nor GPI anchoring of the protein is sufficient to confer a signaling activity on a membrane protein, and emphasize the specificity of the response to PrP^c engagement.

The effect of PrP^c engagement on Ca^{2+} fluxes and on Src tyrosine kinase activation clearly implicate it in basic signaling events in lymphocytic cells. Fyn does not seem to be responsible for the activation observed here. Furthermore, our observations emphasize the importance of PrP^c localization at the cell surface and the necessity for raft integrity in PrP^c-dependent signal transduction.

The distribution of PrP^c may be partially determined by the GPI anchor [46]. But other reports [22, 47] and this study make clear that the incorporation of GPI-linked proteins into rafts is dependent on several parameters, and is not systematic. It is becoming increasingly obvious that different types of raft-like domains, presenting different patterns of resistance to detergent, contain functionally different GPI proteins [48, 49]. The presence of the GPI anchor indicates the possibility for the protein to move into such structures, perhaps to participate in a signaling pathway [34]. In addition, PrP^c can be considered an atypical GPI-linked protein because its recycling was shown not to depend predominantly on the GPI anchor. PrP^c is delivered to classical endosomes after internalization whereas most of the GPI-linked proteins continuously cycle between the plasma membrane and the Golgi compartment without passing through classical endocytic organelles [50]. However, intracellular signaling pathways, including Ca^{2+} signals or protein phosphorylation, seem to be tightly linked to the mode of lateral distribution of PrP^c. The increase in all of the signals was indeed observed when the majority of PrP^c molecules moved into rafts, and activation of Src protein tyrosine kinases was abolished when rafts were disrupted. In the same context, cross-linking of PrP^c using specific Abs triggered in vivo neuronal apoptosis, suggesting that PrP^c plays a role in the control of neuronal survival [51].

Although abundant data showing PrP^c localization in rafts of resting cells are available, few studies have paid attention to the effect of PrP^c engagement on its association with rafts. However, the transient association of certain proteins with rafts seems to allow regulation of their activity [52]. A study using FRET in Jurkat T cells recently concluded that although GPI-linked proteins are among the most typical components of detergent resistant membrane fractions, GPI anchoring is not sufficient to induce wholesale clustering within small, compact lipid rafts [53]. We observed PrP^c in rafts of resting CEM-T cells but only in one-third of the cells. Most importantly, after PrP^c cross-linking, the proportion of cells where the PrP^c-GM_1 colocalization was observed rose twofold. Discrepancies may be related to the different experimental protocols and cellular models used.

PrP^c localization at the cell surface certainly has an impact on the development of prion diseases. The protease-resistant form (PrP^{Sc}) stems from GPI-anchored PrP^c, but not from the transmembrane counterpart form [54]. Such findings, and another study [55], therefore argue that PrP^{Sc} formation is restricted to specific subcellular compartments, termed caveolae-like domains, a particular category of rafts. More recent data do not support the view that the late endosome/lysosome are primary compartments for PrP^c conversion to PrP^{Sc}. In membrane fusion experiments using polyethylene glycol, conversion of membrane-associated PrP^c to PrP^{Sc} required insertion of PrP^{Sc} seeds into PrP^c-containing membranes. Baron et al. [56] therefore propose that the generation of new PrP^{Sc} during transmissible spongiform encephalopathy infection requires insertion of incoming PrP^{Sc} into the raft domains of recipient cells. This implies that the transconformation process also requires the incorporation of PrP^c into rafts.

In this membrane context, our study suggests that alterations in the signaling pathways associated with PrP^c may have dramatic consequences for the fate of cells with high expression levels of this molecule.

Acknowledgements. This investigation was supported in part by grants from ATC 'Prions', from the Institut National de la Santé et de la Recherche Médicale, and by the Université Louis Pasteur, Strasbourg, France.

1 Aguzzi A. and Weissman C. (1997) Prion research: the next frontiers. Nature **389:** 795–798
2 Prusiner S. B. (1998) Prions. Proc. Natl. Acad. Sci. USA **95:** 13363–13383
3 Barclay G. R., Houston E. F., Halliday S. I., Farquhar C. F. and Turner M. L. (2002) Comparative analysis of normal prion protein expression on human, rodent, and ruminant blood cells by using a panel of prion antibodies. Transfusion **42:** 517–526
4 Liu T., Li R., Wong B. S., Liu D., Pan T., Petersen R. B. et al. (2001) Normal cellular prion protein is preferentially expressed on subpopulations of murine hemopoietic cells. J. Immunol. **166:** 3733–3742
5 Lotscher M., Recher M., Hunziker L. and Klein M. A. (2003) Immunologically induced, complement-dependent up-regulation of the prion protein in the mouse spleen: follicular dendritic cells versus capsule and trabeculae. J. Immunol. **170:** 6040–6047
6 Bueler H., Fischer M., Lang Y., Bluethmann H., Lipp H. P., DeArmond S. J. et al. (1992) Normal development and behaviour of mice lacking the neuronal cell-surface PrP protein, Nature **356:** 577–582
7 Roesler R., Walz R., Quevedo J., de-Paris F., Zanata S. M., Graner E. et al. (1999) Normal inhibitory avoidance learning and anxiety, but increased locomotor activity in mice devoid of PrP(C), Brain Res. Mol. Brain Res. **71:** 349–353
8 Wong B. S., Liu T., Li R., Pan T., Petersen R. B., Smith M. A. et al. (2001) Increased levels of oxidative stress markers detected in the brains of mice devoid of prion protein. J. Neurochem. **76:** 565–572
9 Aguzzi A., Montrasio F. and Kaeser P. S. (2001) Prions: health scare and biological challenge. Nat. Rev. Mol. Cell Biol. **2:** 118–126
10 Aguzzi A., Klein M. A., Montrasio F., Pekarik V., Brandner S., Furukawa H. et al. (2000) Prions: pathogenesis and reverse genetics. Ann. N. Y. Acad. Sci. **920:** 140–157
11 Cashman N. R., Loertscher R., Nalbantoglu J., Shaw I., Kascsak R. J., Bolton D. C. et al. (1990) Cellular isoform of the scrapie agent protein participates in lymphocyte activation. Cell **61:** 185–192
12 Li R., Liu D., Zanusso G., Liu T., Fayen J. D., Huang J. H. et al. (2001) The expression and potential function of cellular prion protein in human lymphocytes. Cell Immunol. **207:** 49–58
13 Fivaz M., Vilbois F., Thurnheer S., Pasquali C., Abrami L., Bickel P. E. et al. (2002) Differential sorting and fate of endocytosed GPI-anchored proteins. EMBO J. **21:** 3989–4000
14 Gorodinsky A. and Harris D. A. (1995) Glycolipid-anchored proteins in neuroblastoma cells form detergent-resistant complexes without caveolin. J. Cell Biol. **129:** 619–627
15 Xavier R., Brennan T., Li Q., McCormack C. and Seed B. (1998) Membrane compartmentation is required for efficient T cell activation. Immunity **8:** 723–732
16 Lewis R. S. (2001) Calcium signaling mechanisms in T lymphocytes. Annu. Rev. Immunol. **19:** 497–521
17 Putney J. W. Jr. (1999) 'Kissin' cousins': intimate plasma membrane-ER interactions underlie capacitative calcium entry. Cell **99:** 5–8
18 Rosado J. A., Porras T., Conde M. and Sage S. O. (2001) Cyclic nucleotides modulate store-mediated calcium entry through the activation of protein-tyrosine phosphatases and altered actin polymerization in human platelets. J. Biol. Chem. **276:** 15666–15675
19 Kunzelmann-Marche C., Freyssinet J. M. and Martínez M. C. (2002) Loss of plasma membrane phospholipid asymmetry requires raft integrity: role of transient receptor potential channels and ERK pathway. J. Biol. Chem. **277:** 19876–19881
20 Venkatachalam K., Rossum D. B. van, Patterson R. L., Ma H. T. and Gill D. L. (2002) The cellular and moleular basis of store-operated calcium entry. Nat. Cell. Biol. **4:** 263–272
21 Naslavsky N., Shmeeda H., Friedlander G., Yanai A., Futerman A. H., Barenholz Y. et al. (1999) Sphingolipid depletion increases formation of the scrapie prion protein in neuroblastoma cells infected with prions. J. Biol. Chem. **274:** 20763–20771
22 Madore N., Smith K. L., Graham C. H., Jen A., Brady K., Hall S. et al. (1999) Functionally different GPI proteins are organized in different domains on the neuronal surface. EMBO J. **18:** 6917–6926
23 Keshet G. I., Bar-Peled O., Yaffe D., Nudel U. and Gabizon R. (2000) The cellular prion protein colocalizes with the dystroglycan complex in the brain. J. Neurochem. **75:** 1889–1897
24 Bonin A. von, Huhn J. and Fleischer B. (1998) Dipeptidylpeptidase IV/CD26 on T cells: analysis of an alternative T-cell activation pathway. Immunol. Rev. **161:** 43–53
25 Luo H., Yu G., Wu Y and Wu J. (2002) EphB6 crosslinking results in costimulation of T cells. J. Clin. Invest. **110:** 1141–1150
26 Wang X. M., Djordjevic J. T., Kurosaka N., Schibeci S., Lee L., Williamson P. et al. (2002) T-cell antigen receptor peptides inhibit signal transduction within the membrane bilayer. Clin. Immunol. **105:** 199–207
27 Kascsak R. J., Rubenstein R., Merz P. A., Tonna-DeMasi M., Fersko R., Carp R. I. et al. (1987) Mouse polyclonal and monoclonal antibody to scrapie-associated fibril proteins. J. Virol. **61:** 3688–3693
28 Aupeix K., Hugel B., Martin T., Bischoff P., Lill H., Pasquali J. L. et al. (1997) The significance of shed membrane particles during programmed cell death in vitro, and in vivo, in HIV-1 infection. J. Clin. Invest. **99:** 1546–1554
29 Martínez M. C., Martin S., Toti F., Fressinaud E., Dachary-Prigent J., Meyer D. et al. (1999) Significance of capacitative Ca^{2+} entry in the regulation of phosphatidylserine expression at the surface of stimulated cells. Biochemistry **38:** 10092–10098
30 Kunzelmann-Marche C., Freyssinet J. M. and Martínez M. C. (2001) Regulation of phosphatidylserine transbilayer redistribution by store-operated Ca^{2+} entry: role of actin cytoskeleton. J. Biol. Chem. **276:** 5134–5139
31 Fasolato C. and Nilius B. (1998) Store depletion triggers the calcium release-activated calcium current (ICRAC) in macrovascular endothelial cells: a comparison with Jurkat and embryonic kidney cell lines. Pflugers Arch. **436:** 69–74
32 Ma H. T., Patterson R. L., Rossum D. B. van, Birnbaumer L., Mikoshiba K. and Gill D. L. (2000) Requirement of the inositol trisphosphate receptor for activation of store-operated Ca^{2+} channels. Science **287:** 1647–1651
33 Bishara N. B., Murphy T. V. and Hill M. A. (2002) Capacitative Ca(2+) entry in vascular endothelial cells is mediated via pathways sensitive to 2 aminoethoxydiphenyl borate and xestospongin C. Br. J. Pharmacol. **135:** 119–128
34 Mattei V. Garofalo T., Misasi R., Circella A., Manganelli V., Lucania G. et al. (2004) Prion protein is a component of the multimolecular signaling complex involved in T cell activation. FEBS Lett. **560:** 14–18
35 Yancey P G., Rodrigueza W. V., Kilsdonk E. P. C., Stoudt G. W., Johnson W. J., Phillips M. C. et al. (1996) Cellular cholesterol efflux mediated by cyclodextrins: demonstration of kinetic pools and mechanism of efflux. J. Biol. Chem. **27:** 16026–16034
36 Kenworthy A. K., Petranova N. and Edidin M. (2000) High-resolution FRET microscopy of cholera toxin B-subunit and GPI-anchored proteins in cell plasma membranes. Mol. Biol. Cell **11:** 1645–1655
37 Brown D. R., Qin K., Herms J. W., Madlung A., Manson J., Strome R. et al. (1997) The cellular prion protein binds copper in vivo. Nature **390:** 684–647
38 Tobler I., Gaus S. E., Deboer T., Achermann P., Fischer M., Rulicke T. et al. (1996) Altered circadian activity rhythms and sleep in mice devoid of prion protein. Nature **380:** 639–642
39 Brown D. R. (2001) Prion and prejudice: normal protein and the synapse. Trends Neurosci. **24:** 85–90

40 Chiarini L. B., Freitas A. R., Zanata S. M., Brentani R. R., Martins V. R. and Linden R. (2002) Cellular prion protein transduces neuroprotective signals. EMBO J. **21:** 3317–3326
41 Mouillet-Richard S., Ermonval M., Chebassier C., Laplanche J. L., Lehmann S., Launay J. M. et al. (2000) Signal transduction through prion protein. Science **289:** 1925–1928
42 Diomede L., Sozzani S., Luini W., Algeri M., De Gioia L., Chiesa R. et al. (1996) Activation effects of a prion protein fragment [PrP-(106–126)] on human leucocytes. Biochem. J. **320:** 563–570
43 Filatov A. V., Shmigol I. B., Kuzin I. I., Sharonov G. V. and Feofanov A. V. (2003) Resistance of cellular membrane antigens to solubilization with Triton X-100 as a marker of their association with lipid rafts – analysis by flow cytometry. J. Immunol. Methods **278:** 211–219
44 Fragoso R., Ren D., Zhang X., Su M. W., Burakoff S. J. and Jin Y. J. (2003) Lipid raft distribution of CD4 depends on its palmitoylation and association with Lck, and evidence for CD4-induced lipid raft aggregation as an additional mechanism to enhance CD3 signaling. J. Immunol. **170:** 913–921
45 Monleon I., Martinez-Lorenzo M. J., Anel A., Lasierra P., Larrad L., Pineiro A. et al. (2000) CD59 cross-linking induces secretion of APO2 ligand in overactivated human T cells. Eur. J. Immunol. **30:** 1078–1087
46 Harder T., Scheiffele P., Verkade P. and Simons K. (1998) Lipid domain structure of the plasma membrane revealed by patching of membrane components. J. Cell Biol. **141:** 929–942
47 Mayor S., Rothberg K. G. and Maxfield F. R. (1994) Sequestration of GPI-anchored proteins in caveolae triggered by cross-linking. Science **264:** 1948–1951
48 Edidin M. (2001) Shrinking patches and slippery rafts: scales of domains in the plasma membrane. Trends Cell. Biol. **11:** 492–496
49 Munro S. (2003) Lipid rafts: elusive or illusive? Cell **115:** 377–388
50 Magalhaes A. C., Silva J. A., Lee K. S., Martins V. R., Prado V. F., Ferguson S. S. et al. (2002) Endocytic intermediates involved with the intracellular trafficking of a fluorescent cellular prion protein. J. Biol. Chem. **277:** 33311–33318
51 Solforosi L., Criado J. R., McGavern D. B., Wirz S., Sanchez-Alavez M., Sugama S. et al. (2004) Cross-linking cellular prion protein triggers neuronal apoptosis in vivo. Science **303:** 1514–1516
52 Lucero H. A. and Robbins P. W. (2004) Lipid rafts – protein association and the regulation of protein activity. Arch. Biochem. Biophys. **426:** 208–224
53 Glebov O. O. and Nichols B. J. (2004) Lipid raft proteins have a random distribution during localized activation of the T-cell receptor. Nat. Cell. Biol **6:** 238–243
54 Kaneko K., Vey M., Scott M., Pilkuhn S., Cohen F. E. and Prusiner S. B. (1997) COOH-terminal sequence of the cellular prion protein directs subcellular trafficking and controls conversion into the scrapie isoform. Proc. Natl. Acad. Sci. USA **94:** 2333–2338
55 Taraboulos A., Scott M., Semenov A., Avrahami D., Laszlo L., Prusiner S. B. et al. (1995) Cholesterol depletion and modification of COOH-terminal targeting sequence of the prion protein inhibit formation of the scrapie isoform. J. Cell Biol. **129:** 121–132
56 Baron G. S., Wehrly K., Dorward D. W., Chesebro B. and Caughey B. (2002) Conversion of raft associated prion protein to the protease-resistant state requires insertion of PrP-res (PrP(Sc)) into contiguous membranes. EMBO J. **21:** 1031–1040